

AUTONOMOUS PHOTOVOLTAIC LIGHTING SYSTEM

Ahmed A. A. Hafez¹, Daniel Montesions-Miracle², and Antoni Sudria-Andreu²

¹Electrical Engineering Department, Faculty of Engineering, Assiut University, Assiut, Egypt, PO 71516 elhafez@aun.edu.eg

² Centre d'Innovació Tecnològica en Convertidors Estàtics i Accionaments (CITCEA-UPC), Departament d'Enginyeria Elèctrica, Universitat Politècnica de Catalunya.ETS d'Enginyeria Industrial de Barcelona, Av. Diagonal, 647,Pl. 2. 08028 Barcelona, Spain

(Received January 4, 2012 Accepted February 7, 2012)

This paper introduces a comparison between the conventional and Photovoltaic (PV) lighting systems. A simple sizing procedure for a PV stand-alone system was advised. The paper also proposes a novel PV lighting system. The proposed system is simple, compact and reliable. The system operation was investigated by thoroughly mathematical and simulation work.

I. INTRODUCTION

Traditionally the power required for illuminating the intra-cities roads is imported from the utility grid. This grid lighting system has a number of disadvantages, such as [1-7]:

- i. It increases the consumption/depletion of fossil fuels and hence energy prices.
- ii. It adds to the environment pollution through the waste products from the power plant [8].
- iii. It worsens the grid stability, and mandates the applications of costly power factor/static var compensators, as a considerable portion of the street lamps has very low lag power factors (0.5-0.65), particularly gas discharge lamps.
- iv. The lighting grid system generally is unreliable, as a fault in/near a single pole may disable the entire road [9-11].

To eradicate these disadvantages, a move toward a lighting system based on the PV is necessary. The PV lighting system has a number of advantages, such as:

- i. Energy independence and environmental compatibility, the fuel is free, and no noise or pollution is created from operating the PV system [1-3].
- ii. The PV lighting system is decoupled from the grid, which enhance the grid stability [11].
- iii. In the PV lighting system, each pole is fully decoupled from the remaining poles. Thus a fault in pole or a group of poles has minimal impact on the entire lighting system, which boosts the safety and the reliability.

This paper introduces a comparison between the grid and the PV lighting system. Also, it proposes a novel PV lighting system.

The paper is organized as follows: Section II introduces a comparison between lighting systems supplied from the grid and the PV modules. The comparison includes a simple sizing procedure for a stand-alone PV system. An innovative PV lighting system was advised in Section III. This Section includes also a detailed modeling for

the different components of the proposed system. Section VI introduces the proposed control technique. The simulation results over the full operating cycle of the advised lighting system are given in Section V.

II. COST COMPARISON

In order to assess the economic visibility of the PV lighting system, a cost comparison between conventional and PV lighting systems is carried out for one kilometer (km) of the road connecting Aswan and Alexandria in Egypt. This road is extended in southern desert in Egypt for around 1,000 km. Egypt in general has nearly sunny climate over the entire year, particularly in the southern desert. Moreover, there are no natural or artificial obstacles that could limit the falling irradiation on the prospect PV system in this road.

A. Conventional System

Different types of lamps are utilized for lighting public avenues and roads in Egypt. However, Halogen Sodium (400W) and Mercury vapor (250W) are widely used, particularly in lighting the intra-cities roads. Recently, there is a move toward replacing these lamps by the Compact Fluoresce Lamp (CFL) (105W) [12].

Usually highways in Egypt are illuminated from the dusk until dawn; thus the street lamp is operating for around 10 hours. The power consumptions of the Halogen, Sodium and CFL lamps in kiloWatt-hour (kWh) for 10 hour operation per day for 20 years are given in Fig. 1. The time span of 20 years is considered in producing Fig. 1 to allow comparison with the PV systems. As the reported average life-cycle of a PV system varies from 20 to 25 years [1-3]. It is worth to mention that some components in the PV system such as batteries, lighting accessories and converters have reduced life cycle than the PV module; however the cost of these components represents around (10% to 15%) of the entire system cost [13-15].

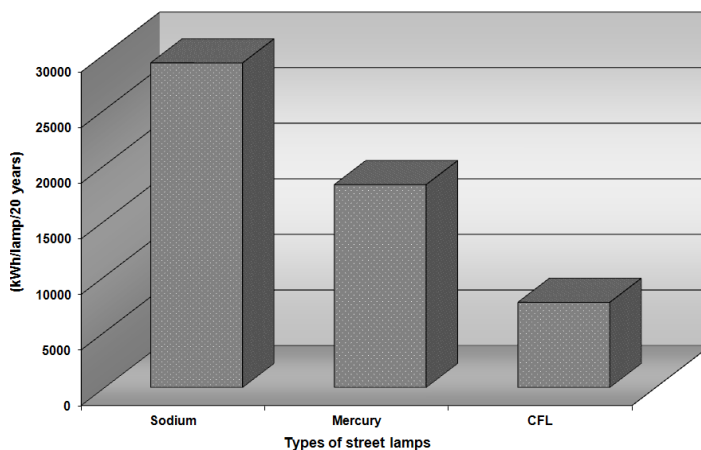


Fig. 1. Power consumption of different types of street lamps in 20 year per one lamp

Figure 1 shows that the CFL consumes around 74% and 49% less than Sodium and Mercury lamps respectively. This energy saving may overwhelm the demerits of

CFL in polluting the grid with harmonics, particularly CFL with conventional ballast [16].

According to the Egyptian code [17], the number of poles per km varies from 30 to 35. An average value of 32 poles per km is taken in this study.

The power consumptions of one-km in the road under concern in kWh per 20 years for Sodium, Mercury and CFL lamps are given in Fig. 2 for 10 hour operation.

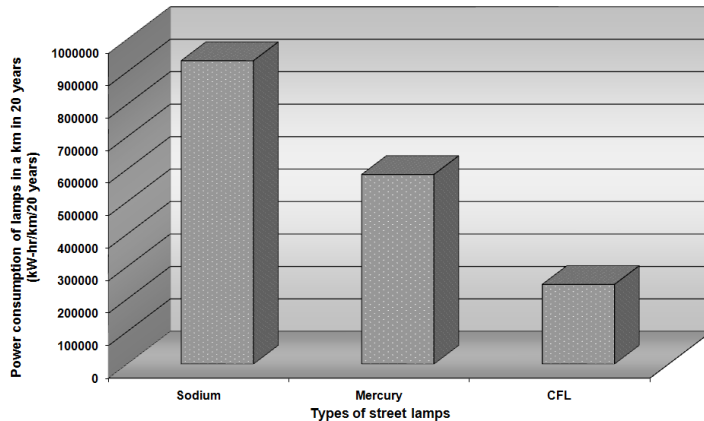


Fig. 2. Power consumption of different lamps in one-km in 20- year

Figure 2 indicates that the required power for illuminating a kilometer in a road over 20 years is around 934.4MWh, 584MWh, and 245.280MWh for Sodium, Mercury and CFL lamps respectively.

The costs of illuminating a distance of one kilometer of the road under concern in 20 years calculated based on the tariff of 0.1US\$/kWh for Sodium, Mercury and CFL are given in Fig. 3. The tariff of 0.1US\$/kWh is taken as an average over the 20 years. However, the cost of 0.1US\$/kWh is considered to be underestimation for prices of electricity generated by fossil fuels in the future [17,18,20].

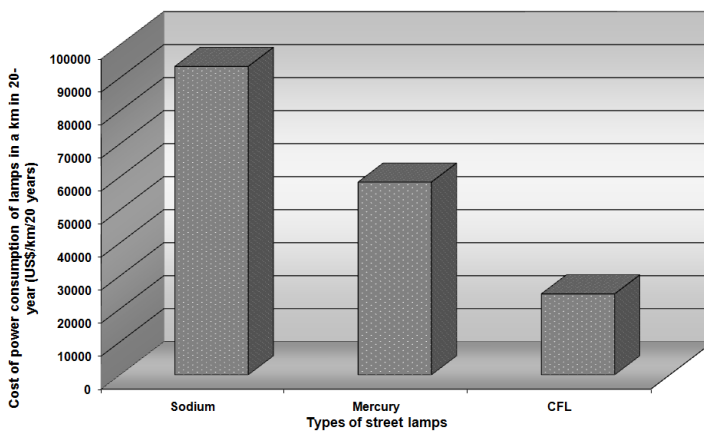


Fig. 3. Cost of power consumption of different lamps in one-km in 20- year

The cost of illuminating a kilometer in the road under concern for 20 years is 93.4 thousand US\$ for Sodium lamp as shown in Fig. 3; therefore, for a road extending

up to 1000km, the cost will be around 100 million US\$, and this is significant, particularly for developing countries.

In developing Fig. 3 the following are ignored:

- i. The impact of electricity production in polluting the surrounding environment and distorting the ecosystem in the nearby rivers/lakes
- ii. The cost due to the consequences of losing lighting system in a busy traffic and condensed roads on the economic.
- iii. The costs of poles, transformers, transmission lines, lamps and protective and auxiliary components

B. PV System

In order to estimate the cost of PV lighting system, the designing process of the system has to be carried out. Generally, the design of a robust PV stand-alone system is iterative procedure that entails a number of steps as shown in Fig. 4.

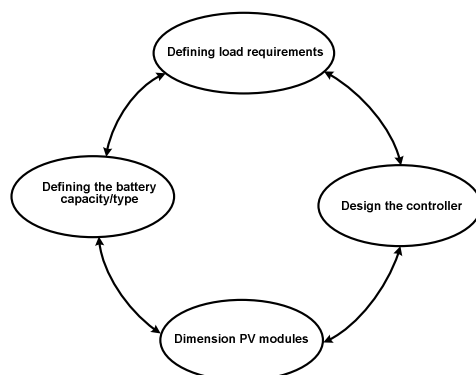


Fig. 4. Flowchart for stand-alone PV system design

i. Load Requirements

The load is the key element in sizing a stand-alone PV system; therefore it desirable to enhance the efficiency of the load. For the system under consideration, it could be realized by selecting more efficient light sources, improved luminaries design, adequate control of operating time/level and better aiming and distribution of the light. Commonly, the load is expressed in terms of ampere-hour (Ah).

For a PV lighting system, the duration of the light availability varies according to the geographical location. The number of night hours could be estimated for an arbitrary site by [18],

$$H_N = 2 \left[12 - \frac{1}{15} \cos^{-1} \left(\frac{-\tan(L)}{\tan(\sin^{-1}(0.397 * \cos(0.9586(N-173)))} \right) \right] \quad (1)$$

where L is the latitude in degree, N Julian day number (1-365). For Egypt and countries near equator, equal length for the day and the night could be fair assumption.

The average daily lighting load is usually calculated for critical design month, where maximum load operation period occurs.

For the system under consideration, the load requirements could be determined as follow; the 105W lamp will be used at voltage of 12VDC. This is the battery voltage, at which the system operates if the battery and load interfacing converter fails. The load current accordingly is 8.75A. As mentioned before that Egypt approximately has equal day and night period throughout the year. Thus, for a lighting system operates between dusk and dawn, the average operating time is 10 hours; and hence the average daily lighting load is 87.5Ah.

ii. Battery Requirements

Battery size is determined according to the maximum allowable discharge depth, derating factor for low temperatures and the desired length of battery stand-alone mode. Deep discharge cycle batteries are commonly used in PV lighting system. The capacity Q of the battery in the lighting system could be estimated from the following empirical formula [18],

$$Q = \frac{\text{length of stand-alone mode(days)} * \text{Average daily load (Ah)}}{\text{Discharge depth} * \text{low temperature derating factor}} \quad (2)$$

The low temperature deteriorates the performance of the battery. This is attributed to the electrochemical process. The phenomenon of low temperature is quite obvious in the Lead-Acid batteries. Their capacities drop by around 20% for the temperature drops from 25°C to 0°C [13-16].

For the proposed PV lighting system, Egypt is a sunny climate throughout the year particularly in the desert where the road under concern is located. However, the stand-alone battery mode is assumed to be 2days. The discharge depth is 80%, and the derating factor due to temperature deviation and aging is assumed to be 0.8 due to desert climate; thus the capacity of the required battery according to (2) is 27.3Ah.

iii. PV Arrangement

The size of the PV modules is commonly estimated based on ability of the system of proving adequate energy to the average daily load for lowest solar insolation levels. The losses in the different parts of the system as well as the impact of temperature rise on the output of the PV module should be considered during the sizing.

The size of PV modules is usually selected according to the solar radiation for the critical design month, where sun insolation is at lowest. The size of the PV could be determined by the following empirical relation [18],

$$\text{PV system rating} = \frac{\text{daily load in Ah} * \text{Average daily load (Ah)}}{\text{System efficiency} * \text{Derating Factor}} \quad (3)$$

The derating factor accounts for reduction in PV output due to temperature, aging and degradation.

For the proposed system, the average daily load is 87.5Ah; and the losses are assumed to be 15% ; derating factor is assumed to 0.7; therefore the size of PV system is around 150W for each pole.

The cost of a 150W PV module is around 600\$ [19]. The cost of batteries, converter and accessories is assumed 50% of PV module cost [4], to consider their

reduced life cycle and the need for their replacement up to four times during the course of system operation.

The cost of illuminating one kilometer in a road for the grid and the PV lighting systems is shown in Fig. 5. For the grid lighting system, the cost is calculated by multiplying the consumed power of the CFL lamps in a kilometer in the road under concern for 20 years by the tariff of 0.1US \$/kWh. For the PV lighting system, the cost is computed by multiplying the cost of the PV system for one pole in the number of poles in a kilometer.

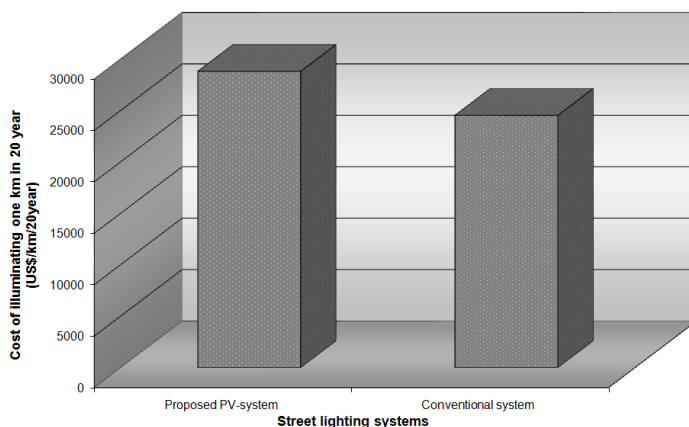


Fig. 5: Cost of illuminating one-kilometer for conventional and PV lighting systems

Figure 5 shows that the cost of PV system is around 16% higher than conventional systems. However the tariff of 0.1\$/kWh used for generating Fig. 5 is underestimation for energy price over the next decades. This as mentioned before is attributed to the steady increase in the price of fossil and the depletion of its reserve.

II. PROPOSED PV LINGHTING SYSTEM

Schematic diagram of the proposed system is shown in Fig. 6,

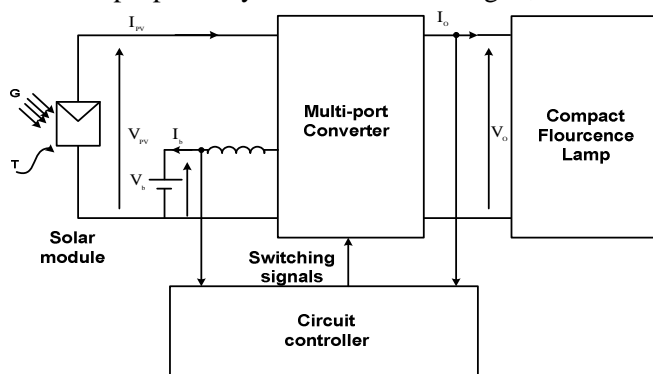


Fig. 6. Proposed PV lighting system per pole

The proposed PV lighting system as shown in Fig. 6 consists of a PV module of 150W, Multi-Port Converter (MPC), battery, and DC lamp of 105W. The detailed design of each component is given in the following sections.

1. PV Generator

Different models are proposed for simulating a PV cell, these models vary in accuracy and complexity. In the proposed system, moderate model is advised for depicting the static and dynamic performance of the PV cell. The PV cell is modeled as a solar irradiation and temperature dependent current source I_{ph} in parallel with diode. This combination is in series with a series resistance R_s [20]. This model of the PV has the advantages of accuracy, robustness and simplicity.

Basically the PV cells are grouped in series to deliver a reasonable voltage/power, these structures are themed modules. The module has an equivalent circuit similar to that of the cell.

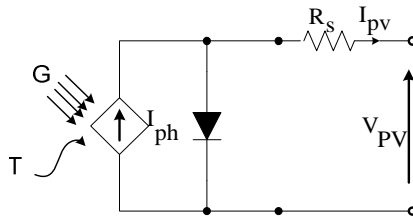


Fig. 7. Equivalent circuit of PV cell/module

The relation between the terminal current I_{pv} and voltage V_{pv} of a PV module is expressed in terms of the terminal voltage V_{pv} , short-circuit current I_{sc} and open-circuit voltage V_{oc} of the module by,

$$I_{pv} = I_{sc} \left(1 - \exp\left(\frac{V_{pv} - V_{oc} + I_{pv} R_s}{V_{th}}\right) \right) \quad (4)$$

where R_s is the series resistance; $V_{th} = nN_s kT/q$ is thermal voltage of the module; n , N_s , K , T and q are ideality factor, number of cells in series, Boltzmann constant and electron charge respectively. The short-circuit current I_{sc} and open-circuit voltage V_{oc} are commonly supplied by the manufacturers at standard conditions.

The PV generator in the proposed PV lighting system is composed of two series connected BP 75W modules. The parameters of BP 75W module are given in Table 1 [21]. Implementing the PV generator from two series connected PV module ensures that the input voltage is higher than battery (output) voltage; thus the MPC operates the PV generator at maximum power point irrespective to irradiation level.

TABLE I
PARAMETERS OF BP 75W SOLAR MODULE AT 25°C AND 1000W²M⁻²[21]

Short circuit current	4.86A
Open circuit voltage	21.6V
Current at Maximum Power Point (MPP)	4.36A
Voltage at MPP	17.2V
Maximum power	75W
Voltage coefficient	-0.08V/C°
Current coefficient	0.65mA/C°
Dimensions	836x670mm

2. Multi-Port Converter

The MPC is a novel topology that is derived from buck and boost topologies, Fig. 8. This circuit allows bidirectional power flow regarding the battery, and unidirectional power flow regarding the PV module and the load.

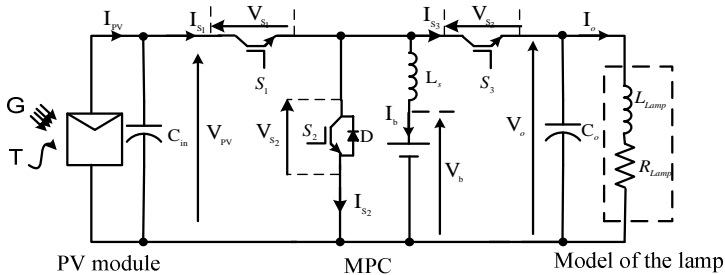


Fig. 8. PV generator, MPC and lamp

For the application under consideration, the power of the PV generator is transferred to the battery, then from the battery to the load through MPC. The MPC can, however, allow dual input/output modes. For example, the PV generator supplies the battery and load simultaneously in dual output mode, while the load could be powered from the battery and PV generator simultaneously in dual input mode. Furthermore, the battery supplies the load, if the source is off.

The MPC ensures that the PV generator operates at its maximum power point irrespective to solar irradiation and temperature. Also it could regulate either the load voltage or current.

The MPC consists of three switches and a diode S_1 , S_2 , S_3 and D . For the application under concern, when S_1 is functioning, S_2 and S_3 are disabled and vice versa. The switch S_1 is normally operated with diode D to charge the battery during the day. They constitute a buck converter, while switches S_2 and S_3 resembles boost converter, and operate during the night to interface the battery to the lamp. The switching diagram of the MPC for the application under the concern is shown in Fig. 9.

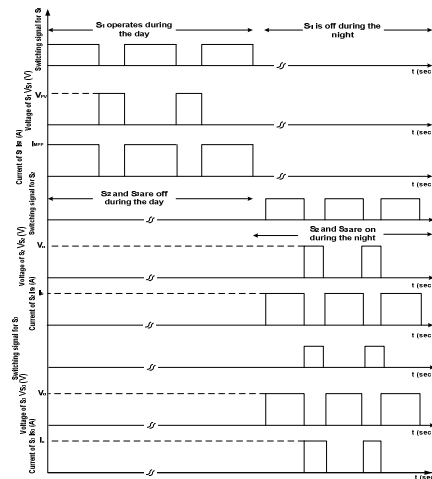


Fig. 9. Switching diagram for the MPC

3. Battery

The battery is the key component for a robust stand-alone PV system, due to its functionality in storing the power extracted from the PV module, operating the load at stable voltages and establishing suitable operating voltages to maximize the captured power from the PV module.

Recently, battery industry has reached a reasonable matured level; different types/capacities of batteries are commercially produced. These differ widely regarding design, performance characteristics and suitability to particular application. The Lead-Acid batteries are commonly deployed in PV applications due availability in different sizes, reduced cost and robust performance [12-15]. Among Lead-Acid batteries, Lead-Antimony type has the advantages of reduced cost, wide availability, good deep charge/discharge cycle, and withstanding high temperature. However Lead-Antimony batteries suffer from the water loss and requirement for albeit high maintenance rate, which can add to the cost of the system.

Due to the orbital motion of the earth, the duration of solar irradiance availability varies considerably according to the geographical locations. Thus, the battery capacity/size varies from site to site for a PV lighting system. However, for Egypt, almost there is a symmetry regarding the length of the day/night over the year. Thus, the batteries in the proposed PV lighting system are more likely not subjected to irregular charging/discharging pattern.

The battery is modeled here as a controlled voltage source in series with a resistor R_b , Fig. 10; the resistor stands for the ohmic losses inside the battery and at the leads [15].

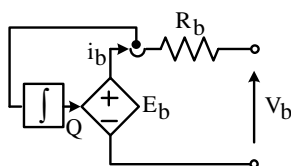


Fig. 10. Model of the battery

The resistance R_b is assumed to remain constant, the voltage E_b is given by,

$$E_p = E_o - V_r \frac{Q}{Q_o} + V_e \exp\left(-\frac{Q_o - Q}{Q_e}\right) \quad (5)$$

where E_o , V_r , V_e are open-circuit, polarization and exponential voltages respectively; Q , Q_o , and Q_e , are current, rated and exponential capacities in terms of ampere-hour respectively.

To supply the required capacity for the system under concern, five Lead-Antimony batteries of 55Ah are connected in parallel, the nominal voltage of each battery is 12V. The battery consists of six-cell; the parameters of a battery cell are given in Table 2, [22].

TABLE 2
PARAMETERS OF UNIT IN A LEAD-ANTIMONY BATTERY [22]

Nominal voltage	2V
Rated capacity	9.2Ah
Internal resistance	0.02Ω

4. Lamp

Due to the growing interest in PV applications, a number of lamps were emerged recently. These lamps operate from a DC source; they could be fitted in variety of applications as lighting. The lamp considered in this work is 105W cool white CFL lamp. This lamp produces around 6800lumens and is modeled as a resistor and an inductor in series. A capacitor is added in parallel to maintain the output voltage constant [9-11]. The CFL lamp in the proposed PV lighting system operates from 120V DC source.

IV. PROPOSED CONTROLLER

For the application under consideration, the MPC charges the battery through S_1 and D during the availability of solar insolation, while the remaining switches are off. During the night, the battery powers the load through switches S_2 and S_3 while switch S_1 is off. The MPC could be considered here as decoupled buck and boost converters. The buck converter charges the battery from the PV module, while the boost converter interfaces the battery and the load. Thus each converter could be controlled independently.

Variety of Maximum Power Point Tracking (MPPT) algorithms are reported in literature [23-25]. These techniques vary according to complexity, cost, hardware implementation and availability. For the PV lighting system, a cheap and efficient MPPT has to be deployed. The incremental conductance MPPT has the advantages of availability and capability of tracking MPP under wide operating conditions of solar irradiance and temperature. The slope of power-voltage curve of a PV generator could be expressed by,

$$\frac{dP_{pv}}{dV_{pv}} = I_{pv} + V_{pv} \frac{dI_{pv}}{dV_{pv}}, \quad (6)$$

The slope of power-voltage curve of a PV module, is positive on the left of MPP, negative on the right and zero at MPP. Thus the relation between the incremental and instantaneous conductance is given by,

$$\begin{aligned} \frac{\Delta I_{pv}}{\Delta V_{pv}} &> -\frac{I_{pv}}{V_{pv}}, \text{ left MPP} \\ \frac{\Delta I_{pv}}{\Delta V_{pv}} &= -\frac{I_{pv}}{V_{pv}}, \text{ at MPP} \quad , \\ \frac{\Delta I_{pv}}{\Delta V_{pv}} &< -\frac{I_{pv}}{V_{pv}}, \text{ right MPP} \end{aligned} \quad (7)$$

MPP is tracked by continuously comparing the incremental and instantaneous conductance and incrementing/decrementing the PV voltage/current. [25]. An innovative implementation for the incremental conductance is proposed in [24]. According to (6), the sum of the incremental and instantaneous conductance is equal to zero at MPP; therefore employing a sufficiently fast PI controller ensures that sum is settled at zero at different operating conditions of temperature and solar irradiance.

$$E = \frac{\Delta I_{pv}}{\Delta V_{pv}} + \frac{I_{pv}}{V_{pv}}, \quad (8)$$

The bandwidth of this controller should be sufficient high to allow satisfactory tracking for solar irradiation [24]. The proposed incremental conductance could be implemented by a low cost DSP.

The parameters of the PI controller tuned using the approach in [24] are given in Table 3.

TABLE 3
PARAMETERS OF PI CONTROLLER IN MODIFIED INCREMENTAL
CONDUCTANCE [24]

Gain	500
Zero	0.4 rad/sec

Placing the zero of the PI controller near to natural origin pole increases the bandwidth, while maintaining the stability and providing sufficient attenuation for the switching frequency ripples.

To prevent the overcharge or excessive discharge of the battery, its voltage is restricted within a band around the nominal value, 12V. The switch S_1 will be opened, if the battery voltage exceeds the upper limit, 14.2V; whereas switches S_2 and S_3 are opened for lower limit violation, 11.1V.

During the load operation, the switches S_2 and S_3 are controlled so that the load voltage is maintained constant at 120V. Although a PI controller is used to regulate the load voltage, however, for the lighting load supplied through the battery an open loop control for the switches will be simple, inexpensive, reliable and sufficient.

The parameters of the PI controller used for regulating the lighting voltage load are tuned using pole-placement technique [26]. The parameters are given in Table 4.

TABLE 4
PARAMETERS OF PI CONTROLLER [BB]

Gain	0.02
Zero	100 rad/sec

V. RESULTS AND DISCUSSIONS

The following figures show the dynamic performance of the system during a complete operating cycle. The solar irradiance was stimulated to vary as half sinusoidal wave, its peak occurs at 12 O'clock; while the PV temperature is maintained constant at 25°C. The solar irradiance and power of PV generator are shown in Fig. 11. Fig. 12 shows the PV generator current and voltage; while Fig. 13 illustrates battery voltage, current, load voltage and power over complete charging and discharging cycle. In Figs. 11-13 solar irradiation is assumed to be available over 12hours from 6 AM until 6 PM, while the lighting system operates over 10 hours from 7 PM until 5 AM.

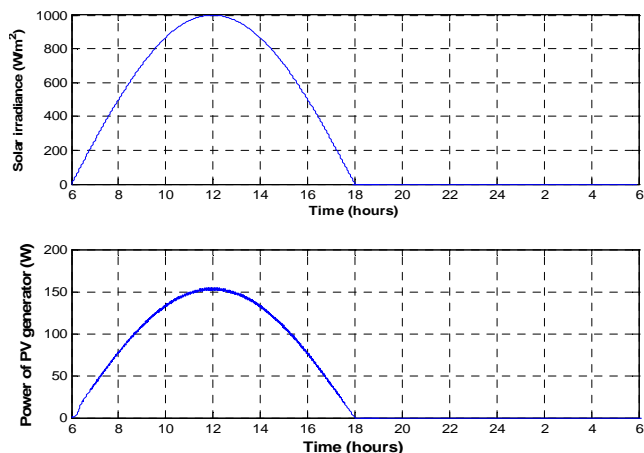


Fig. 11. Top graph: Solar irradiance, Bottom graph: PV generator power over a full operating cycle and at 25°C

Figure 11 shows that the proposed MPPT forces the system to operate at MPP at varying irradiation. The PV generator power varies almost linearly with the solar irradiance; while the terminal voltage is nearly constant. This conclusion was reported in [24].

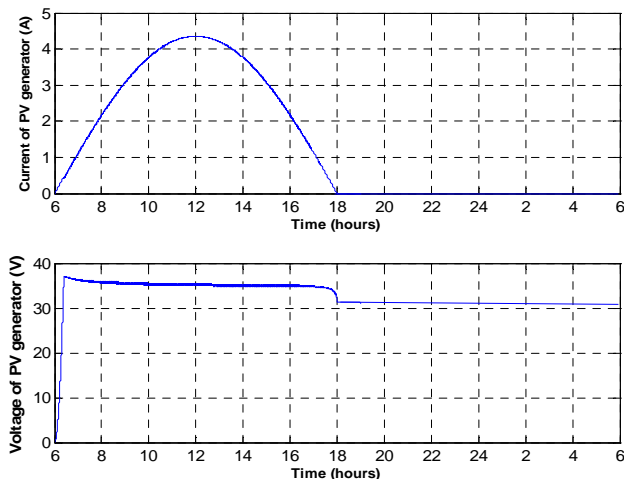


Fig. 12. Top graph: PV generator current, Bottom graph: PV generator voltage over a full operating cycle and at 25°C

Figure 12 shows that the current of PV generator also varies linearly with the solar irradiance; this could be understood from (4). The PV generator short circuit current I_{sc} is function solar irradiance dependent.

The PV generator terminal voltage has non zero value in the absence of solar irradiance, Fig. 12. This is attributed to the characteristics of solar cell which resembles P-N junction. In the absence of solar irradiance, this P-N junction is reserve based, thus there is potential gradient. The PV module usually consists of large number of series connected cells, 36 for the BP 75W. The sum of the reverse voltage of all these cells gives the non-zero value of the PV generator terminal voltage.

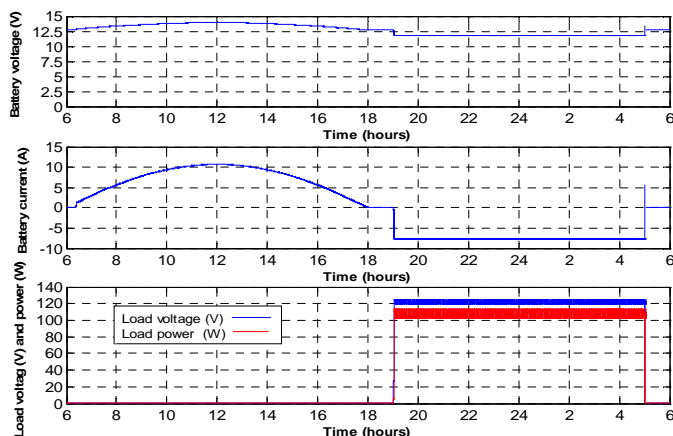


Fig. 13. Top graph: battery voltage (blue); Middle graph: battery current; Bottom graph: load power (blue) and voltage (red) over a full operating cycle and at 25°C

Figure 13 shows that the lighting operates from dusk (7PM) until dawn (5AM), which is more convenient for Egypt and countries near equator. Limiting the duration of PV lighting operation without comprising safety and reliability is a priority in stand-alone PV systems. There are two hours over the operating cycle, where all switches of MPC are off.

Figure 13 shows that the battery voltage is within the allowed limits. The boost stage of the MPC increases the load voltage to a level, which is suitable for DC or AC lighting structures.

The MPC as shown in Figs. 12 and 13 have the advantages of providing continuous, ripple-free, battery and load currents. However, the input current of PV generator is discontinuous and a filter capacitor has to be deployed.

VI. CONCLUSION

The following conclusions could be drawn:

1. The CFL is proven to be future trendsetter for the lighting industry due to the reduced power consumption and extended lifetime; however this lamp is albeit expensive.
2. The cost of PV lighting system is slightly higher than their conventional counterparts; however the merits of reliability, sustainability and environmentally compatibility overwhelm the evaluated cost.
3. The proposed MPPT tracks the MPP under different levels of solar irradiance
4. At reduced level of solar insolation, the tracking efficiency of the proposed MPPT is quite poor.
5. The Lead-Acid batteries are widely adopted in PV applications due availability in different sizes, reduced cost and robust performance.
6. Lead-Antimony battery enjoys reduced cost, wide (availability, good deep charge/discharge cycle, and withstanding high temperature, whereas they suffer from the water loss and requirement for albeit high maintenance rate.
7. The proposed MPC is simple, reliable and efficient.

8. The proposed MPC has the advantages of reducing the distortion in the PV generator, battery and load currents, which limits the losses and increases the life-cycle of these components.
9. The proposed MPC has prominent advantage of producing high level DC output, which could be suitable for further AC conversion.
10. The proposed PV lighting system has the advantages of reliability, simplicity and environmental compatibility.

ACKNOWLEDGMENT

The authors are acknowledged for the Spanish Agency of International Development Cooperation (AECID) for funding this research work under A/030852/10.

REFERENCES

- [1] T. J. Bialasiewicz, "Power-Electronics Systems for the Grid Integration of Renewable Energy Sources: A Survey " *IEEE Transactions on industrial Electronics*, vol. 53, p. 1002:1016, August 2006.
- [2] T. J. Bialasiewicz, "Renewable Energy System with Photovoltaic Power Generators: Operation and Modeling," *IEEE Transactions on industrial Electronics*, vol. 55, pp. 2752-2758, July 2008.
- [3] E. Endo and K. Kurokawa "Sizing procedure for photovoltaic systems " in *IEEE First World Conference on Photovoltaic Energy Conversion*, 1994, pp. 1196 - 1199.
- [4] V. Risser and H. Post "Stand-Alone Photovoltaic Systems: A Handbook of Recommended Design Practices." *Sandia PV Design Assistance Center*, SAND87-7023, November 1991.
- [5] J. F. Kreider and F. Kreith "Solar Energy Handbook", McGraw-Hill, 1981.
- [6] M. G. Villalva; J. R. Gazoli and E. R. Filho. "Comprehensive Approach to Modeling and Simulation of Photovoltaic Arrays," *IEEE Transactions on power electronics*, vol. 24, pp. 1198-1208, 2009.
- [7] A. D. Hansen; P. Sørensen; L. H. Hansen and H. Bindner "Models for a Stand-Alone PV System", Risø-R-1219(EN) / SEC-R-12, 2000
- [8] S. Hameed; R. D. Cess and J. S. Hogan; " Response of the Global Climate to Changes in Atmospheric Chemical Composition Due to Fossil Fuel Burning" *Journal of Geophysical*, vol. 85, 1980, pp. 7537-7545.
- [9] IES Lighting Handbook, 8th ed., Reference and Application, Illuminating Engineering Society of North America, New York, 1993.
- [10] American National Standard Practice for Roadway Lighting, ANSI/IES RP-8, Illuminating Engineering Society of North America, 1983.
- [11] S. Rios; R. Castaneda and D. Veas "Harmonic distortion and power factor assessment in city street gas discharge lamps" *IEEE Transaction on Power Delivery*, vol. 11, pp: 1013-1020, April 1996.
- [12] Reference about the street lamps in Egypt and the future trendsetter
- [13] J. B. Copetti and F. Chenlo" Lead/acid batteries for photovoltaic applications: Test results and modeling" *Journal of Power Sources*, vol. pp. 109-118, January 1994.

- [14] D. U. Sauera; M. Bächler; G. Boppa, W. Höheb, J. Mittermeierb, P. Sprauc, B. Willerd and M. Wollnyd" Analysis of the performance parameters of lead/acid batteries in photovoltaic systems" *Journal of Power Sources*, vol. 64, pp. 197-201, January-February 1997.
- [15] IEEE Recommended Practice for Installation and Maintenance of Lead-Acid Batteries for Photovoltaic Application; NASI/IEEE Std 973-1987.
- [16] R. R. Verderber; O. C. Morse and W. R. Alling "Harmonics from compact fluorescent lamps" *IEEE Transaction on Industry Application*, vol. 29, pp. 670-674, May/June 1993.
- [17] Egyptian Minsitry of Electricity and Energy" Regulation for lightings of Public avaenu and Roads" internal memorandum, April 1990.
- [18] J. Dunlop" Stand-alone Photovoltiac lighting system" *Florida University Engery research Centre publications*, pp. 1-25, September 1998
- [19] Solar direct, <http://www.solardirect.com/pv/pvlist/pvlist.htm>
- [20] M. G. Villalva; J. R. Gazoli, and E. R. Filho, "Comprehensive Approach to Modeling and Simulation of Photovoltaic Arrays," *IEEE Transactions on Power Electronics*, vol. 24, pp. 1198-1208, 2009.
- [21] BP 75W <http://www.connexaenergy.com/Default.aspx?tabid=933&CategoryID=299&List=0&SortField=ProductName%2cProductName&Level=a&ProductID=516>
- [22] D. A. J. Rand" Vave-Regulated Lead-Acid Batteries" 1st edition, Library of Congress, 2004.
- [23] A. A. Hafez "simple and robust Maximum Power Point Tracking Algorithm for a solar cell," in *World Congress on Electronics and Electrical Engineering (WCEEENG'10)*, 2010,pp. 240-245, April 2010.
- [24] A. A. Hafez; D. Montesions and A. Sudria " *Autonmoinous Cascaded PV system*" *Journal of Engineering Sciencs*, vol. 1, pp. 243-250, November 2011
- [25] T. Efram and P. L. Chapman " Comparison of Photovoltiac Array Maximum Power Point Tracking Techniques" *IEEE Transactions on Energy Conversion*, vol. 22, 2007.
- [26] W. Dorf and R. Bishop, "Modern Control Systems", 2nd edition Addison-Wesley, 1998.

نظام فعال للإضاءة باستخدام الألواح الشمسية

انتوتي سودري اندريه

دانيال منسنوس ميكيل

أحمد عبدالملك عبدالحافظ

الملخص العربي :

يقدم هذا البحث مقارنة بين نظم الإضاءة التي تستمد الكهرباء من الشبكة الكهربائية وتلك التي تعتمد علي الألواح الشمسية. يحتوي البحث علي طريقة بسيطة لتحديد المكونات اللازمة لنظام ألواح شمسية مستقل . كما يقدم البحث نظام جديد لإضاءة الطرق الدولية . هذا النظام بسيط التصميم ، محكم وذا اعتمادية عالية . تم التحقق من أداء النظام المقترح عن طريق تحليل رياضي وعمل محاكاة مضني .